Spin Echoes*†

E. L. HAHN‡
Physics Department, University of Illinois, Urbana, Illinois
(Received May 22, 1950)

Intense radiofrequency power in the form of pulses is applied to an ensemble of spins in a liquid placed in a large static magnetic field H_0. The frequency of the pulsed r-f power satisfies the condition for nuclear magnetic resonance, and the pulses last for times which are short compared with the time in which the nutating macroscopic magnetic moment of the entire spin ensemble can decay. After removal of the pulses a non-equilibrium configuration of isochromatic macroscopic moments remains in which the moment vectors precess freely. Each moment vector has a magnitude at a given precession frequency which is determined by the distribution of Larmor frequencies imposed upon the ensemble by inhomogeneities in H_0. At times determined by pulse sequences applied in the past the constructive interference of these moment vectors gives rise to observable spontaneous nuclear induction signals. The properties and underlying principles of these spin echo signals are discussed with use of the Bloch theory. Relaxation times are measured directly and accurately from the measurement of echo amplitudes. An analysis includes the effect on relaxation measurements of the self-diffusion of liquid molecules which contain resonant nuclei. Preliminary studies are made of several effects associated with spin echoes, including the observed shifts in magnetic resonance frequency of spins due to magnetic shielding of nuclei contained in molecules.

I. INTRODUCTION

In nuclear magnetic resonance phenomena the nuclear spin systems have relaxation times varying from a few microseconds to times greater than this by several orders of magnitude. Any continuous Larmor precession of the spin ensemble which takes place in a static magnetic field is finally interrupted by field perturbations due to neighbors in the lattice. The time for which this precession maintains phase memory has been called the spin-spin or total relaxation time, and is denoted by T_2. Since T_2 is in general large compared with the short response time of radiofrequency and pulse techniques, a new method for obtaining nuclear induction becomes possible. If, at the resonance condition, the ensemble at thermal equilibrium is subjected to an intense r-f pulse which is short compared to T_2, the macroscopic magnetic moment due to the ensemble acquires a non-equilibrium orientation after the driving pulse is removed. On this basis Bloch[1] has pointed out that a transient nuclear induction signal should be observed immediately following the pulse as the macroscopic magnetic moment precesses freely in the applied static magnetic field. This effect has already been reported[2] and is closely related to another effect, given the name of "spin echoes," which is under consideration in this investigation. These echoes refer to spontaneous nuclear induction signals which are observed to appear due to the constructive interference of precessing macroscopic moment vectors after more than one r-f pulse has been applied. It is the purpose of this paper to describe and analyze these effects due to free Larmor precession in order to show that they can be applied for the measurement of nuclear magnetic resonance phenomena, particularly relaxation times, in a manner which is simple and direct.

II. FEATURES OF NUCLEAR INDUCTION METHODS

(A) Previous Resonance Techniques (Forced Motion)

The chief method for obtaining nuclear magnetic resonance has been one whereby nuclear induction signals are observed while an ensemble of nuclear spins is perturbed by a small radiofrequency magnetic field. A large d.c. magnetic field $\bar{H}_0$ establishes a net spin population at thermal equilibrium which provides a macroscopic magnetic moment $\bar{M}_0$ oriented parallel to $\bar{H}_0$. The forced motion of $\bar{M}_0$ is brought about by subjecting the spin ensemble to a rotating radiofrequency field $\bar{H}_1$ normal to $\bar{H}_0$ at the resonance condition $\omega=\omega_0=\gamma H_0$, where γ is the gyromagnetic ratio, ω is the angular radiofrequency, and ω_0 is the Larmor frequency. The techniques which obtain resonance under this condition provide for the application of a driving r-f voltage to an LC circuit tuned to the Larmor frequency. The sample containing the nuclear spins is placed in a coil which is the inductance of the tuned circuit. At resonance a small nuclear signal is induced in the coil and is superimposed upon an existing r-f carrier signal of relatively high intensity. In order to detect this small nuclear signal the r-f carrier voltage is reduced to a low level by a balancing method if the LC circuit is driven by an external oscillator,[1,3] or the LC circuit may be the tuned circuit of an oscillator which is designed to change its level of operation when nuclear resonance absorption occurs.[4,5] In general, a condition exists whereby transitions induced by H_1, which tend

* This research was supported in part by the ONR.
† Reported at the Chicago Meeting of the American Physical Society, November, 1949; Phys. Rev. **77**, 746 (1950).
‡ Present address: Physics Dept. Stanford University, Stanford, California.
[1] F. Bloch, Phys. Rev. **70**, 460 (1946).
[2] E. L. Hahn, Phys. Rev. **77**, 297 (1950).
[3] Bloembergen, Purcell, and Pound, Phys. Rev. **73**, 679 (1948).
[4] R. V. Pound, Phys. Rev. **72**, 527 (1947); R. V. Pound and W. D. Knight, Rev. Sci. Inst. **21**, 219 (1950).
[5] A. Roberts, Rev. Sci. Inst. **18**, 845 (1947).

to upset the thermal equilibrium of the spins, are in competition with processes of emission due to lattice perturbations which tend to restore equilibrium. Spin relaxation phenomena, which are measured in terms of the relaxation times T_2 and T_1 (spin-lattice), must be distinguished simultaneously from effects due to the influence of r-f absorption. Consequently the study of resonance absorption line shapes, intensities, and transients must carefully take into account the intensity of H_1 and the manner in which resonance is obtained.

In practice, resonance takes place over a range of frequencies determined by the inhomogeneity of H_0 throughout the sample. For resonances concerning nuclei in liquids it is generally found that the natural line width given by $1/T_2$ on a frequency scale is much narrower than the spread in Larmor frequencies caused by external field inhomogeneities, whereas the converse is true in solids. Therefore steady state resonance lines due to nuclei in liquids are artificially broadened; transient signals are modified in shape and have decay times which are shorter than would otherwise be determined by T_1 and T_2.

(B) Nuclear Induction Due to Free Larmor Precession

The observation of transient nuclear induction signals due to free Larmor precession becomes possible at the resonance condition described above if the r-f power is now applied in the form of intense, short pulses. The r-f inductive coil which surrounds the sample is first excited by the applied pulses and thereafter receives spontaneous r-f signals at the Larmor frequency due to the precessing nuclei. In particular, the echo effect is brought about by subjecting the sample to two r-f pulses in succession (the simplest case) at pulse width $t_w < \tau < T_1, T_2$, where τ is the time interval between pulses. At time τ after the leading edge of the second pulse the echo signal appears. Since H_1 is absent while these signals are observed, no particular attention need be given to elaborate procedures for eliminating receiver saturation effects (as must be done in the forced motion technique) providing that T_2 is large enough to permit observation of echoes at times when the receiver has recovered from saturation due to the pulses. Because the T_2 of nuclei in liquids is generally large enough to favor this condition, the technique for obtaining echoes in this work has been largely confined to the magnetic resonance of nuclei in liquid compounds. Preliminary observations of free induction signals in solids, where T_2 becomes of the order of microseconds, indicate again, however, that procedures must be undertaken for preventing receiver saturation due to intense pulses.

For spin ensembles in liquids it will be shown that the analysis of observed echo signals yields direct information about T_1 and T_2 without requiring consideration of the effect of H_1 on the measured decay of the signal. Because of the inhomogeneity in H_0, the self diffusion of "spin-containing liquid molecules" brings about an attenuation of observed transient signals in addition to the decay due to T_1 and T_2. However, this is only serious for liquids of rather low viscosity which also have a large T_2 for the resonant nuclei concerned, whereas in conventional resonance methods (forced motion), field inhomogeneities obscure a direct measurement of T_2 in liquids over a much wider range of viscosities. The free motion technique, which will hereafter be denoted by the method of spin echoes or free nuclear induction, also reveals in a unique manner differences in resonant frequency between nuclear spins of the same species located in different parts of a single molecule or in different molecules. Such differences have been observed by previous resonance methods,[6,7] and the echo technique gives at least as good a resolution in the measurement of small shifts.

In this investigation the in-phase condition of a precessing spin ensemble is considered to be eventually destroyed because of lattice perturbations which limit the phase memory time of Larmor precession. The precession of an individual spin may be interrupted either because its energy of precession is transferred to neighboring spins in a time $\sim T_2''$ (mutual spin-spin flipping), or because this energy is transferred to the lattice as thermal energy in a time $\sim T_1$. The spread in Larmor frequencies, due to local "z magnetic field" fluctuations at the position of the nucleus caused by neighboring spins and paramagnetic ions, also serves to disturb phase memory (H_0 is in the z direction). In a formal treatment[3] this effect is considered in conjunction with the interaction giving rise to T_2'', and a general relaxation time T_2' is formulated. The inverse of the total relaxation time, $1/T_2 \sim 1/T_2' + 1/T_1$, therefore becomes the uncertainty in frequency of a precessing spin, which can then acquire an uncertainty in phase of the order of one radian in time T_2.

It will be convenient to describe the formation of free induction signals by considering the free precession of individual macroscopic moment vectors $\bar{M}_0(\omega_0)$. Each of these vectors has a magnitude at a given ω_0 which is determined by a z magnetic field distribution imposed upon the ensemble by inhomogeneities in H_0. In this spectral distribution $\bar{M}_0(\omega_0)$ can be defined as an isochromatic macroscopic moment which consists of an ensemble of nuclear moments precessing in phase at the assigned frequency ω_0. The precessional motion of any $\bar{M}_0(\omega_0)$ vector about the total magnetic field (with or without r-f pulses) can be followed regardless of what phases the individual isochromatic moments have with respect to one another throughout the entire spectrum. At the time a short r-f pulse initiates the free precession of $\bar{M}_0(\omega_0)$ from a classically non-precessing initial condition at thermal equilibrium, relaxation and possibly diffusion processes begin to diminish the magnitude of

[6] W. G. Proctor and F. C. Yu, Phys. Rev. **77**, 717 (1950).
[7] W. C. Dickinson, Phys. Rev. **77**, 736 (1950).

the precessing vector $\bar{M}_0(\omega_0)$ as the individual nuclear spins get out of phase with one another or return to thermal equilibrium.

The actual H_0 field which persists at the position of a precessing spin accounts for a given ω_0 and hence for a given $\bar{M}_0(\omega_0)$. In liquids this persisting field and the way it is distributed over the sample is taken to be entirely due to the magnet; any contributions to the local field at the nucleus by neighbors in the lattice average out in a time short compared to a Larmor period. Free induction signals from nuclei in solids, however, indicate that a broad distribution in H_0 exists (compared to a relatively homogeneous external field) which is determined by fixed lattice neighbors, and now this local field distribution does not average out.

The description of free induction effects is simplified by transforming to a coordinate system in which the $x'y'$ plane (Fig. 1) is rotating at some convenient reference angular frequency ω'. This frequency is usually chosen to be the center frequency of a given distribution of isochromatic moments, where the distribution is typically described by a Gaussian or Lorentz (damped oscillator) function. In the next section definite properties of the rotating coordinate representation are presented. The precessional motion as viewed in the rotating system is conveniently followed when (1) $\bar{M}_0(\Delta\omega)$ undergoes forced transient motion during the driving pulse, and (2) when the $\bar{M}_0(\Delta\omega)$ vectors precess freely, where $\Delta\omega=\omega_0-\omega'$ and $\bar{M}_0(\omega_0)=\bar{M}_0(\Delta\omega)$. The condition in (1) has already been analyzed theoretically and experimentally.[8,9,10] Although it is strictly a condition in which $\bar{M}_0(\Delta\omega)$ precesses about the total field $\bar{H}_0+\bar{H}_1$, as viewed in the laboratory system, it has been characterized by the fact that not only does $\bar{M}_0(\Delta\omega)$ appear to precess about the z axis at a high Larmor frequency, but also it appears to nutate with respect to the z axis at a much lower frequency.[11]

III. THEORY AND APPLICATIONS

(A) The Moving Coordinate Representation

Consider the torque equation, with no damping, which describes the precession of $\bar{M}$ as seen in the laboratory system:

$$d\bar{M}/dt=\gamma(\bar{M}\times\bar{H}), \tag{1}$$

where $\bar{H}$ is the total magnetic field. During the application of r-f pulses, $\bar{H}=\bar{H}_0+\bar{H}_1$; and during the free precession of $\bar{M}$ in the absence of pulses, $\bar{H}=\bar{H}_0$. During a pulse it is convenient to transform to a moving coordinate system in which $\omega'=\omega$, and $\bar{H}_1$ is chosen to lie along the x' axis. It will be pointed out, however, that, regardless of the choice of direction of $\bar{H}_1$ in the $x'y'$ plane, the description of the spin echo model presented later is not affected, except under a very special condition. If $D\bar{M}/dt$ is the observed torque in the moving coordinate system, then by a well-known transformation,

$$d\bar{M}/dt=D\bar{M}/dt+\bar{\omega}\times\bar{M}, \tag{2}$$

where $\bar{M}\equiv M(u, v, M_z)$ and $\bar{H}\equiv H(H_1, 0, H_0)$. Combining (1) and (2) we obtain

$$D\bar{M}/dt=\bar{M}\times(\Delta\bar{\omega}+\bar{\omega}_1) \tag{3}$$

as the torque in the moving system during a pulse. The vector $\bar{M}$ is identified with the isochromatic moment $\bar{M}_0(\Delta\omega)$ which appears to precess about the effective field vector $(\Delta\bar{\omega}+\bar{\omega}_1)/\gamma$. Let $(\Delta\omega)_{\frac{1}{2}}$ be the width at half-maximum of an assumed function which describes the distribution of $\bar{M}_0(\Delta\omega)$ over the inhomogeneous external field, and let ω' be the center frequency of this distribution. If, during a pulse, the inequality $1/t_w$, $\omega_1\gg(\Delta\omega)_{\frac{1}{2}}$ applies at resonance ($\omega\approx\omega'$), then the precession of any $\bar{M}_0(\Delta\omega)$ vector will appear to take place practically about the $\bar{\omega}_1$ vector in the moving system. This precessional frequency is given by $\omega_1=\gamma H_1$ (of the order of kilocycles) which appears in the laboratory system as a frequency of nutation superimposed upon a high Larmor precession frequency ($\sim$30 Mc). In the rotating system any $\bar{M}_0(\Delta\omega)$ vector will precess in a cone whose axis is in the direction of $\bar{H}_1$ and whose angle is determined by the angle between $\bar{M}_0(\Delta\omega)$ and $\bar{H}_1$ at the time $\bar{H}_1$ is suddenly applied. When $\bar{H}_1$ is suddenly removed, the vector $\bar{M}_0(\Delta\omega)$ is oriented at a fixed angle θ with respect to the z axis, and precesses freely at angular frequency $\Delta\omega$ about the effective magnetic field $\Delta\bar{\omega}/\gamma$ along the z axis. The angle θ will be determined by $\omega_1 t_w$ and the initial conditions established by successive pulses applied in the past.

(B) Simple Vector Model of the Spin Echo

For spin ensembles in liquids a simple vector model will account for the manner in which two applied r-f pulses establish a given spectral distribution of moment components in the $x'y'$ plane, where the axis of the inductive coil is oriented. This distribution then freely precesses to form, by constructive interference, a resultant "echo" in the $x'y'$ plane. This is formulated by integrating a general expression for the $x'y'$ component of the isochromatic moment over all frequencies $\Delta\omega$ imposed by H_0 field inhomogeneities. Purcell[12] has suggested a three-dimensional model of the echo, Fig. 1, which arises in a special case. At $t=0$, when $\bar{H}_1$ is suddenly applied, $\bar{M}_0(\Delta\omega)$ is at thermal equilibrium, aligned parallel to $\bar{H}_0$ along the z axis. During time t_w

[8] N. Bloembergen, *Nuclear Magnetic Relaxation* (Martinus Nijhoff, The Hague, 1948).
[9] H. C. Torrey, Phys. Rev. **76**, 1059 (1949).
[10] E. L. Hahn, Phys. Rev. **76**, 461 (1949).
[11] This is observed to come about in the laboratory system as the resonance absorption mode becomes modulated at the low nutation frequency. Classically speaking, the term nutation is applied only to the physical top, in which the presence of angular momentum about an axis other than the spin axis is responsible for the nutation. Although a nuclear spin possesses extremely negligible angular momentum about any axis other than its spin axis, the term nutation is convenient to retain here in order to refer to the tipping motion of $\bar{M}_0(\Delta\omega)$ with respect to the z axis.
[12] Private communication.

of the first pulse, let $\bar{M}_0(\Delta\omega)$ precess an angle $\omega_1 t_w=\pi/2$ about $\bar{H}_1$, so that all moment vectors in the spectrum will have nutated into the $x'y'$ plane. Let $\tau\gg 1/(\Delta\omega)_{\frac{1}{2}}$, $T_1=T_2=\infty$, and assume a rectangular spectrum over $\Delta\omega$, i.e., $g(\Delta\omega)=$const., where $g[(\Delta\omega)_{\frac{1}{2}}]=0$. During time $t_w\leqslant t\leqslant\tau$, the various isochromatic moment pairs $M_0(+|\Delta\omega|)$, $M_0(-|\Delta\omega|)$, will precess at frequency $\Delta\omega$, maintaining a symmetry about the y' axis but rotating in opposite directions. These precessing moments will attain an isotropic distribution in a time $\gtrsim 2\pi/(\Delta\omega)_{\frac{1}{2}}$ prior to which a free induction decay is observed.[2] At time τ the second r-f pulse, identical with the first one, will rotate the moment pairs from angular positions $\varphi=3\pi/2\pm|\Delta\omega|\tau$, $\theta=\pi/2$ to $\varphi=(0,\pi)$, $\theta=\pi-|\Delta\omega|\tau$ in spherical coordinates. During the time interval $\tau+t_w\leqslant t<2\tau$ all moment vectors interfere destructively with one another and distribute themselves isotropically over a unit sphere until the time $t\approx 2\tau$ when they interfere constructively. At time 2τ all of the moment vectors will have again precessed angles $\Delta\omega\tau$ respectively from their positions at $t=\tau+t_w$ so that they terminate in a figure eight pattern whose equation is $\theta=\varphi$. Free induction for $t\gtrsim\tau+t_w$ will be obtained from the linearly polarized component of magnetization

$$v(\Delta\omega,t)=M_0\sin\Delta\omega\tau\sin\Delta\omega(t-\tau) \tag{4}$$

along the y' axis. The observed induction voltage will be due to the integrated precessing moment

$$V(t)=\int_{-(\Delta\omega)_{\frac{1}{2}}}^{(\Delta\omega)_{\frac{1}{2}}} g(\Delta\omega)v(\Delta\omega,t)d(\Delta\omega), \tag{5}$$

where

$$\int_{-(\Delta\omega)_{\frac{1}{2}}}^{(\Delta\omega)_{\frac{1}{2}}} g(\Delta\omega)d(\Delta\omega)=1.$$

Therefore, from (4) and (5) we obtain

$$V(t)=\frac{M_0}{2}\left[\frac{\sin(\Delta\omega)_{\frac{1}{2}}(t-2\tau)}{(\Delta\omega)_{\frac{1}{2}}(t-2\tau)}-\frac{\sin(\Delta\omega)_{\frac{1}{2}}t}{(\Delta\omega)_{\frac{1}{2}}t}\right]. \tag{6}$$

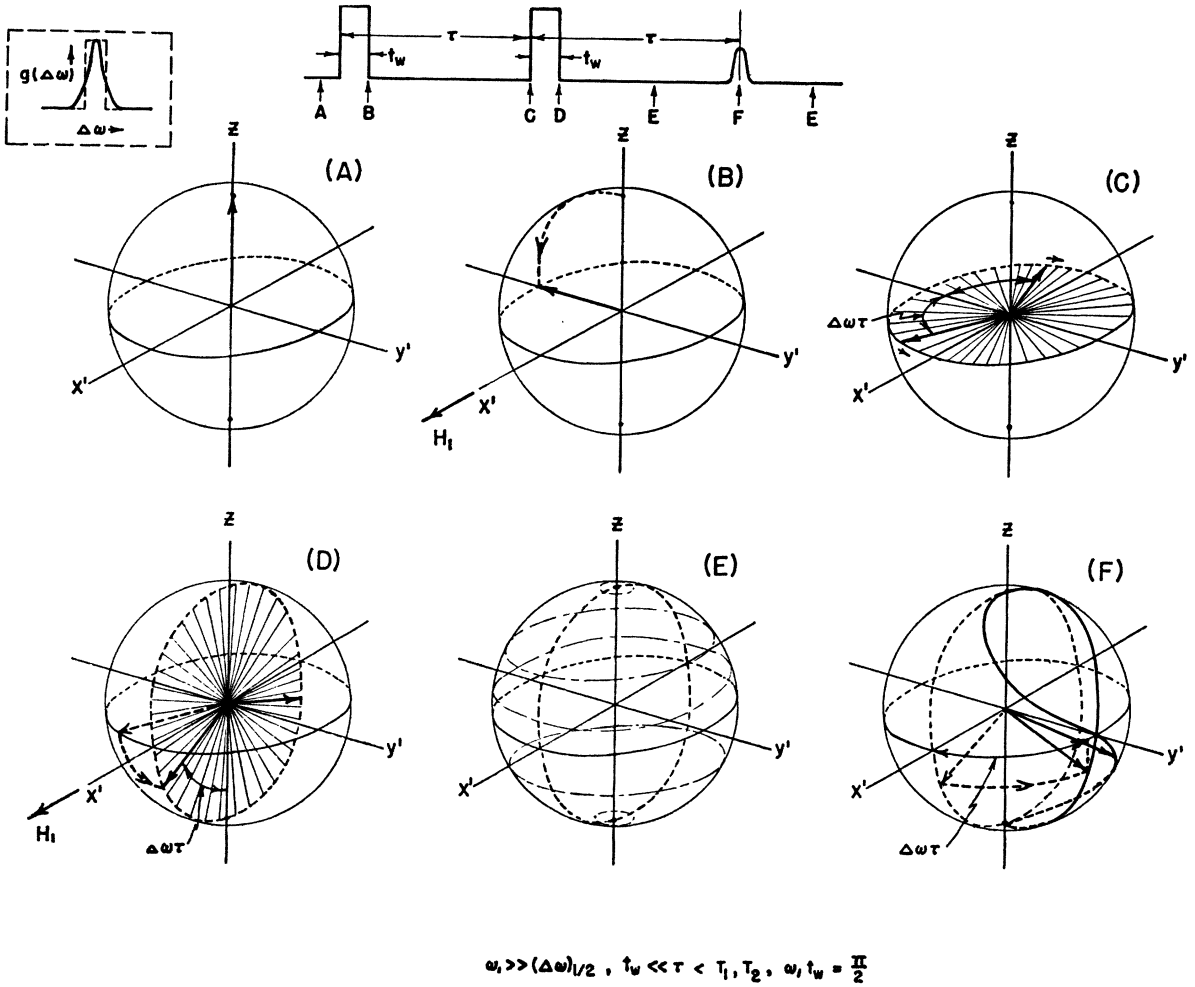

FIG. 1. For the pulse condition $\omega_1 t_w=\pi/2$, the formation of the eight-ball echo pattern is shown in the coordinate system rotating at angular frequency ω. The moment vector monochromats are allowed to ravel completely in a time $\tau\gg 1/(\Delta\omega)_{\frac{1}{2}}$ before the second pulse is applied. The echo gives maximum available amplitude at $\omega_1 t_w=2\pi/3$.

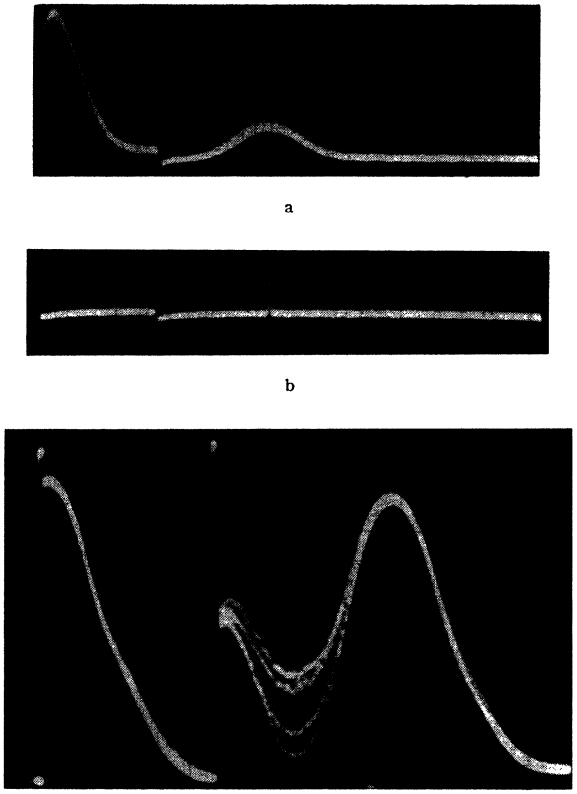

FIG. 2. Oscillographic traces for proton echoes in glycerine. The two upper photographs indicate broad and narrow signals corresponding to H_0 fields of good and poor homogeneity. The pulses, scarcely visible, are separated by 0.0005 sec. The induction decay following the first pulse in the top trace has an initial dip due to receiver saturation. The bottom photograph shows random interference of the induction decay with the echo for several exposures. The two r-f pulses are phase incoherent relative to one another.

According to the first term on the right side of (6) the echo maximum occurs at $t=2\tau$, and the signal lasts for $\sim 4\pi/(\Delta\omega)_{\frac{1}{2}}$ seconds. No free induction is predicted after the second pulse for this particular case, which is illustrated in Fig. 2 (top). For extremely large $(\Delta\omega)_{\frac{1}{2}}$ the echo becomes very sharp and the free induction decay after the first pulse becomes practically unobservable. Equation (6) indicates that periodic maxima should occur at times $2\pi/(\Delta\omega)_{\frac{1}{2}}$ sec. apart during the appearance of free induction signals. These maxima are not observed in general for this reason, because the choice of $g(\Delta\omega)$ here does not correspond to experimental conditions. A modulation is observed in particular cases because of an entirely different effect which will be discussed later.

(C) General Analysis

The echo effect will now be treated in a general way, after which some of the simplifying assumptions outlined for the very simple case just described will be applied. By making use of Bloch's equations[1] and choosing $g(\Delta\omega)$ to approximate the actual distribution of spins over H_0, the decay of echo signals due to T_1, T_2, and self-diffusion (in the case of some liquids) can be accounted for. As in the case illustrated above, $\bar{H}_1$ will be chosen to lie along the x' axis in the rotatir g system for both pulses. Actually $\bar{H}_1$ may appear in any possible position in the $x'y'$ plane during the second pulse since the r-f is not necessarily coherent for both pulses. However, free induction signals will be independent of this random condition as long as $\tau \gg 1/(\Delta\omega)_{\frac{1}{2}}$.[13] This signifies that free induction decay following a single pulse does not interfere with the echo (see Fig. 2, bottom, where this interference effect is shown). Ordinarily the scalar differential equations obtained from (3) are written to include additional torque terms due to relaxation according to Bloch. In the case of echo phenomena it is found that nuclear signals due to precessing nuclear moments contained in liquid molecules (particularly of low viscosity) are not only attenuated by the influence of T_1 and T_2, but also suffer a decay due to self-diffusion of the molecules into differing local fields established by external field inhomogeneities. Consequently, the phase memory of Larmor precession can be destroyed artificially to an appreciable extent. The effect of self-diffusion will be qualitatively accounted for by using Bloch's equations with a diffusion term added:

$$du/dt+[\Delta\omega+\delta(t)]v=-u/T_2 \qquad (7\text{-A})$$

$$dv/dt-[\Delta\omega+\delta(t)]u+\omega_1 M_z=-v/T_2 \qquad (7\text{-B})$$

$$dM_z/dt-\omega_1 v=-(M_z-M_0)/T_1. \qquad (7\text{-C})$$

u and v are the components of magnetization parallel and normal to $\bar{H}_1$ respectively. As time increases from the point where the first pulse is applied, $\delta(t)$ is taken to represent, due to diffusion, the shift in Larmor frequency of the u and v components away from the initial value of $\Delta\omega$. If the decay terms during a pulse are neglected, since t_w is very short compared to all decay time constants, the motion will be simply described by the following solutions of (7):

$$u(t)=(\Delta\omega/\beta)AQ+u(t_i) \qquad (8\text{-A})$$

$$v(t)=A\sin(\beta t+\xi) \qquad (8\text{-B})$$

$$M_z(t)=-(\omega_1 A/\beta)Q+M_z(t_i), \qquad (8\text{-C})$$

where $Q=\cos(\beta t+\xi)-\cos(\beta t_i+\xi)$ and $\beta=[(\Delta\omega)^2+\omega_1^2]^{\frac{1}{2}}$. The constants A, ξ, $u(t_i)$, and $M_z(t_i)$ are determined by initial conditions at the beginning of the pulse $(t=t_i)$ and the assumption that $M_z(t_i)^2+u(t_i)^2+v(t_i)^2=M_z(t)^2+u(t)^2+v(t)^2$ during the pulse. When the r-f pulse is removed at $t=t_i'$, then $\omega_1=0$, and Eqs. (8-A) and

[13] In the calculation which follows, $\bar{H}_1$ during the second pulse could be assumed to have an arbitrary angle α with respect to $\bar{H}_1$ which existed during the first pulse. It can easily be shown that all nuclear signals are independent of α and that the direction of the echo resultant will be at an angle $\alpha+\pi/2$ with respect to the direction of $\bar{H}_1$ which was applied during the second pulse.

(8-B) combine to give a solution

$$F(t)=F(t_i')\exp\{-(t-t_i')/T_2 + i[\Delta\omega(t-t_i')+\int_{t_i'}^{t}\delta(t'')dt'']\}, \quad (9)$$

where $F=u+iv$ and $t\geq t_i'$.

A constant field gradient, $(dH_0/gl)_{Av}=G$, shall be assumed to exist throughout the sample, where l is any direction in which the field gradient has the given average value G. The actual direction of $\bar{H}_0$ must vary in the sample. Any precessing moment which experiences a change in the magnitude of $\bar{H}_0$ due to diffusion will adiabatically follow a corresponding change in Larmor frequency of precession which will take place about the new direction of $\bar{H}_0$. Therefore $\bar{H}_1$ will not have the same magnitude during both pulses for a particular spin because the component of the applied r-f field perpendicular to the different directions of $\bar{H}_0$ will differ. Free induction signals will suffer negligible distortion because of this as compared to the distortion caused by variation in direction and magnitude of $\bar{H}_1$ throughout the sample due to coil geometry. For purposes of simplicity, the analysis will not attempt to take into account any sort of inhomogeneity of the $\bar{H}_1$ field.

In (9) let $\delta(t'')=\gamma Gl(t'')$ and

$$\int_{t_i'}^{t}\delta(t'')dt''=\Phi(t)-\Phi(t_i'), \quad (10)$$

where $\Phi(t)-\Phi(t_i')$ is the total phase shift accumulated in a time $t-t_i'$ by a precessing spin due to diffusion. The solution (9) must be averaged over all Φ, using a phase probability function $P(\Phi, t)$, by considering in particular the integral

$$\int_{-\infty}^{\infty}\{\exp i[\Phi(t)-\Phi(t_i')]\}P(\Phi, t)d\Phi = \exp\left[-\frac{kt^3}{3}-i\Phi(t_i')\right], \quad (11\text{-A})$$

where $k=(\gamma G)^2D$, and D is the self-diffusion coefficient of the spin-containing molecule. It can be shown[14] that

$$P(\Phi, t)=(4\pi kt^3/3)^{-\frac{1}{2}}\exp[-\Phi^2/(4\pi kt^3/3)]. \quad (11\text{-B})$$

From Eq. (7-C) the solution for $M_z[\Delta\omega+\delta(t)]$ must be averaged over the probability that the moment vector corresponding to it is precessing at frequency $\Delta\omega+\delta(t)$ at time t. The ordinary diffusion law will be assumed to apply as regards the distance of diffusion l which corresponds to frequency shift δ. General solutions of (7) representing free motion can therefore be written as follows:

$$F(t)=F(t_i')\exp\{-(t-t_i')/T_2-\tfrac{1}{3}kt^3 + i[\Delta\omega(t-t_i')-\Phi(t_i')]\} \quad (12)$$

$$M_z(t)=M_0\left[1+\frac{M_i-M_0}{M_0}\exp-(t-t_i')/T_1\right], \quad (13)$$

where

$$M_i=\int_{-\infty}^{\infty}M_z(\Delta\omega+\delta, t_i')P(\delta, t)d\delta \quad (14)$$

and[15]

$$P(\delta, t)=\frac{1}{[4\pi k(t-t_i')]^{\frac{1}{2}}}\exp[-\delta^2/4k(t-t_i')].$$

For the case in which twin pulses are applied, we have at $t=0$, $M_z=M_0$ and $u=v=0$. At $t=t_w$ the moments in the rotating system are obtained from (8). At time τ the r-f pulse is again applied and removed at $t=\tau+t_w$. After the second pulse the initial values of the magnetization components which undergo free motion are as follows:

$$u(\tau+t_w)=\frac{\Delta\omega}{\omega_1M_0}[v(\tau)v(t_w)-u(\tau)u(t_w)] + \frac{u(t_w)M_z(\tau)}{M_0}+u(\tau) \quad (15\text{-A})$$

$$v(\tau+t_w)=\frac{v(t_w)}{M_0}\left[M_z(\tau)-\frac{\Delta\omega}{\omega_1}u(\tau)\right]+v(\tau)\cos\beta t_w \quad (15\text{-B})$$

$$M_z(\tau+t_w)=\frac{1}{M_0}[M_z(\tau)M_z(t_w) + u(\tau)u(t_w)-v(\tau)v(t_w)]. \quad (15\text{-C})$$

The v component, which is an even function in $\Delta\omega$, provides the free induction voltage, whereas the u component is an odd function in $\Delta\omega$ and does not contribute to the integral which will be applied in (18). Imposing the condition $\omega_1\gg\Delta\omega$ and $\tau\gg t_w$ we obtain:

(a) $(t\leq\tau)$:

$$v(t, \Delta\omega)\approx -M_0\sin\omega_1t_w\cos\Delta\omega t\exp(-t/T_2-\tfrac{1}{3}kt^3) \quad (16)$$

(b) $(t\geq\tau)$:

$$v(t, \Delta\omega)\approx M_0\sin\omega_1t_w[\sin^2\tfrac{1}{2}\omega_1t_w\cos\Delta\omega(t-2\tau) - \cos^2\tfrac{1}{2}\omega_1t_w\cos\Delta\omega t]\exp(-t/T_2-\tfrac{1}{3}kt^3) - M_z(\tau)\sin\omega_1t_w\cos\Delta\omega(t-\tau) \exp[-(t-\tau)/T_2-\tfrac{1}{3}k(t-\tau)^3]. \quad (17)$$

[14] First one must take into account all possible paths (essentially all possible areas expressed by the integral in (10)) which the diffusing molecule may take in the l, t plane so that the total phase shift accumulated by the precessing spin which the molecule carries with it has a given value which is the same regardless of path length and final position of the molecule. The ordinary diffusion law is assumed to apply in expressing the probability of a given path under the constraint that a certain $\Phi(t)$ be accumulated. The distribution function (11-B) over all phases then follows by applying a standard deviation theorem (see James V. Uspensky, *Introduction to Mathematical Probability* (McGraw-Hill Book Company Inc., New York, 1937), p. 270). The author is indebted to Dr. C. P. Slichter for this derivation.

[15] E. H. Kennard, *Kinetic Theory of Gases* (McGraw-Hill Book Company, Inc., New York, 1938), p. 283.

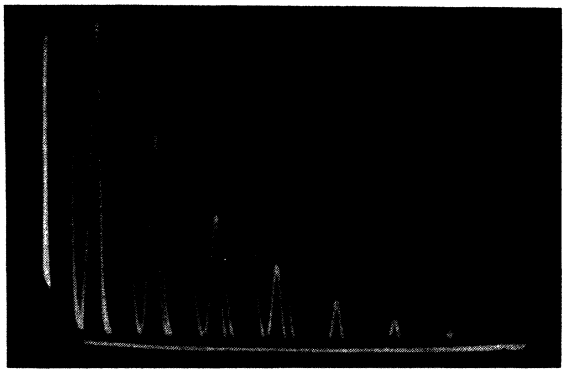

FIG. 3. Multiple exposures of proton echoes in a water solution of $Fe(NO_3)_3$ (2.5×10^{18} Fe^{+++} ions/cc). The faint vertical traces indicate paired pulses which are applied at time intervals $\gg T_2$, with the first pulse of each pair occurring at the same initial position on the sweep. For each pulse pair the interval τ is increased by 1/300 sec. The echoes are spaced 2/300 sec. apart and the measured decay time constant of the echo envelope gives $T_2=0.014$ sec.

The measured signal will be due to the integral

$$V(t)=\int_{-\infty}^{\infty} g(\Delta\omega)v(t,\Delta\omega)d(\Delta\omega). \tag{18}$$

For convenience $g(\Delta\omega)$ is chosen to be a Gaussian distribution:

$$g(\Delta\omega)=(2\pi)^{-\frac{1}{2}}T_2^*\exp[-(\Delta\omega T_2^*)^2/2],$$
$$T_2^*=(2\ln 2)^{\frac{1}{2}}/(\Delta\omega)_{\frac{1}{2}}, \tag{19}$$

where the integral of $g(\Delta\omega)$ over all $\Delta\omega$ is equal to unity. Integration of (16) and (17) according to (18) gives the following:

(a) $(t\leq\tau)$:

$$V(t)\approx -M_0\sin\omega_1 t_w\exp\left[-\left(\frac{t^2}{2T_2^{*2}}+t/T_2+\frac{kt^3}{3}\right)\right], \tag{20}$$

(b) $(t\geq\tau)$:

$$V(t)\approx M_0\sin\omega_1 t_w\left\{\left(\sin^2\frac{\omega_1 t_w}{2}\right)\exp\left[-\frac{(t-2\tau)^2}{2T_2^{*2}}\right]-\left(\cos^2\frac{\omega_1 t_w}{2}\right)\exp\left(-\frac{t^2}{2T_2^{*2}}\right)\right\}$$
$$\times\exp\left(-\frac{kt^3}{3}-t/T_2\right)-M_z(\tau)\sin\omega_1 t_w$$
$$\times\exp-\left[\frac{1}{2}\left(\frac{t-\tau}{T_2^*}\right)^2+\frac{t-\tau}{T_2}+\frac{k}{3}(t-\tau)^3\right]. \tag{21}$$

The echo at $t=2\tau$ is accounted for by the first term in (21) and has a width of $\sim T_2^*$ seconds. The remaining terms in (20) and (21) predict the occurrence of free induction decay signals immediately following the removal of the pulses. Actual shapes of all induction signals are determined mainly by what shape $g(\Delta\omega)$ happens to have due to external field inhomogeneities over the magnet. T_2 will play a significant role in affecting the shape only if $T_2\lesssim T_2^*$. Signal amplitudes are independent of T_2^* as long as $\omega_1\gg 1/T_2^*$. In practice $g(\Delta\omega)$ is roughly a function which is some compromise between the Gaussian distribution given above and the Lorentz damped oscillator function given by

$$g(\Delta\omega)=\frac{2T_2^*}{1+(\Delta\omega T_2^*)^2}\quad\text{where}\quad T_2^*=\frac{1}{(\Delta\omega)_{\frac{1}{2}}}.$$

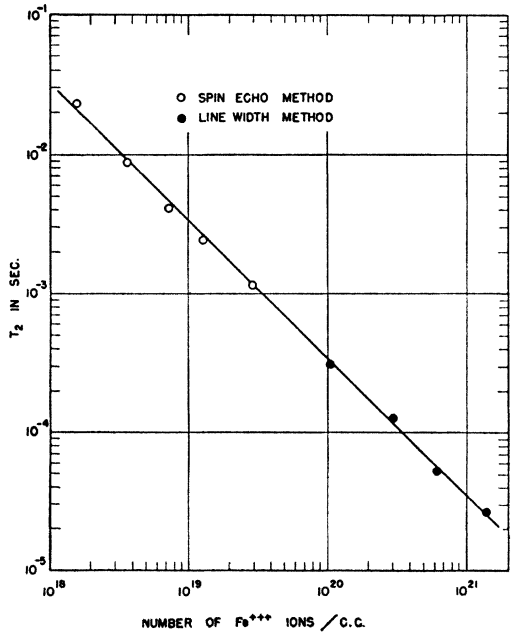

FIG. 4. T_2 measurements from the envelope decay of proton echoes are obtained for given concentrations of $Fe(NO_3)_3$ in H_2O. The plot compares with measurements made by the line width method (see reference 3).

(D) Measurement of T_2

If $\frac{1}{3}kt^3\ll t/T_2$ and $T_2^*\ll\tau<T_2$, T_1, then T_2 can be measured directly by plotting the logarithm of the maximum echo amplitude at $t=2\tau$ *versus* arbitrary values of 2τ. Figure 3 illustrates photographs of echoes on the oscilloscope for protons in a water solution of Fe^{+++} ions under these conditions. Figure 4 indicates how the measured T_2 for various concentrations of Fe^{+++} ions agrees with results obtained by Bloembergen, *et al.*[3] using the line width method. The law $C\propto 1/T_2$ is obeyed where C is the number of Fe^{+++} ions/cc for a given sample.

(E) Secondary Spin Echoes

If a third r-f pulse (identical to pulses producing the primary echo) is applied to the sample at a time T with respect to $t=0$, where $2\tau<T<T_2$, additional echoes occur at the following times: $T+\tau$, $2T-2\tau$, $2T-\tau$, $2T$. For $\tau<T<2\tau$ the signal at $2T-2\tau$ is absent but the others remain (see Fig. 5). These additional echoes can be readily predicted by rewriting Eq. (15) such that $\tau+t_w\rightarrow T+t_w$, $\tau\rightarrow T$, $t_w\rightarrow\tau+t_w$ ($\cos\beta t_w$ remains un-

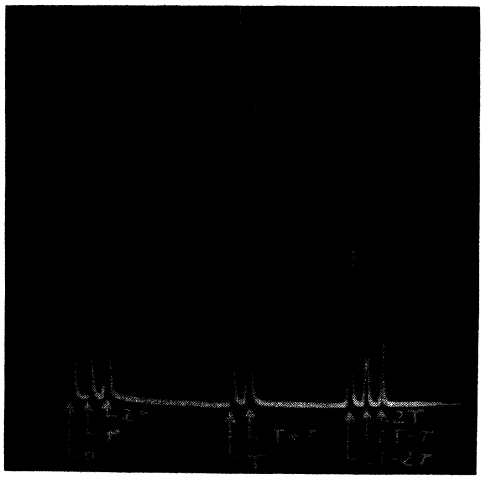

a

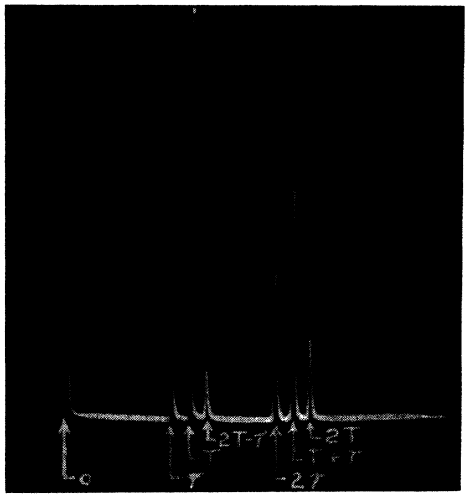

b

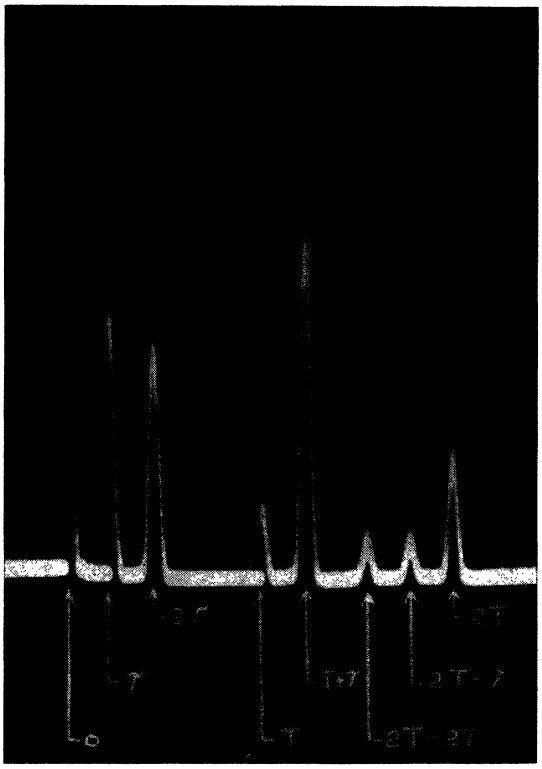

c

FIG. 5. Proton echo patterns in H_2O resulting from three applied r-f pulses. The pulses are visible in the upper two traces, and have a width $t_w \sim 0.5$ msec. In the upper trace $\tau = 0.008$ sec., $T = 0.067$ sec., and for the second trace $\tau = 0.046$ sec. and $T = 0.054$ sec. The bottom photograph shows a similar pattern for the case $T > 2\tau$ where induction decay signals can be seen following very short invisible r-f pulses. Saturation of a narrow band communications receiver, used in the case of the upper two traces, prevents the observation of these signals, whereas a wide band i.f. amplifier makes this observation possible in the bottom photograph.

changed in (15-B)) and applying the resulting expressions as initial conditions in (12), (13), and (14). In this manner, by successive application of accumulating initial conditions, the echo pattern resulting from any number and sequence of r-f pulses can be predicted. After integrating $v(t)$ over $\Delta\omega$ for $t \gtrsim T > 2\tau$, using $g(\Delta\omega)$ according to (19), the following expression for $V(t)$ is obtained (terms due to induction decay directly following the pulse are omitted and assumed not to interfere with the echoes since $\tau \gg T_2^*$):

$$V(t) \approx \frac{M_0}{2}(\sin^3\omega_1 t_w) \times \exp\left\{-(T-\tau)\left(\frac{1}{T_1}-\frac{1}{T_2}\right)-t/T_2 - \frac{k}{3}[\tau^3+(t-T)^3]-k\tau^2(T-\tau) - \frac{[t-(T+\tau)]^2}{2T_2^{*2}}\right\} \quad (22\text{-A})$$

$$-M_0\left(\sin\omega_1 t_w \sin^4\frac{\omega_1 t_w}{2}\right) \times \exp\left\{-\frac{[t-(2T-2\tau)]^2}{2T_2^{*2}}-t/T_2-\frac{kt^3}{3}\right\} \quad (22\text{-B})$$

$$+M_z(\tau)\left(\sin\omega_1 t_w \sin^2\frac{\omega_1 t_w}{2}\right) \times \exp\left\{-\frac{[t-(2T-\tau)]^2}{2T_2^{*2}}-(t-\tau)/T_2 - k(t-\tau)^3/3\right\} \quad (22\text{-C})$$

$$+\frac{M_0}{4}(\sin^3\omega_1 t_w) \times \exp\left\{-\frac{(t-2T)^2}{2T_2^{*2}}-t/T_2-\frac{kt^3}{3}\right\}. \quad (22\text{-D})$$

Term (22-A) provides a "stimulated echo" signal at $T+\tau$. The signal at $2T-2\tau$ (22-B) can be expected qualitatively by considering the "eight ball" alignment

in Fig. 1 as equivalent to an initial orientation of moments in a given direction by an imaginary r-f pulse at 2τ. Therefore, it follows that the stimulating pulse at T causes an "image echo" to occur at $2T-2\tau$. The signals at $2T-\tau$ (22-C) and $2T$ (22-D) are essentially primary echoes corresponding to twin pulses at τ, T and 0, T respectively. The signal at $2T$ is modified by the presence of the second r-f pulse at τ so that it does not have the same trigonometric dependence on $\omega_1 t_w$ as do the primary echoes at τ and $2T-\tau$.[16] Experimentally the various echo signals are observed to go through maxima and minima in general agreement with their respective trigonometric dependences on $\omega_1 t_w$ as this quantity is varied. The stimulated echo at $T+\tau$ is particularly interesting and useful in view of the fact that if τ is sufficiently small so that all terms in the exponent of (22-A) are negligible except T/T_1, the signal survives as long as T_1 permits. The remaining echo signals in liquids of low viscosity have maxima which attenuate in a time much shorter than T_1 as T is arbitrarily increased for a given τ. This is due to the diffusion factor $\frac{1}{3}kl^3$ which occurs in the exponents of (22-B), (22-C), and (22-D), but occurs only as $k\tau^2 T$ in (22-A). This property of the stimulated echo is schematically indicated in Fig. 6. The constructive interference at $T+\tau$ is due to moment vectors which previously existed as $M_z(\Delta\omega)$ components distributed in a spectrum approximately as $\cos\Delta\omega\tau$ during the time interval $\tau+t_w \rightarrow T$. This can be seen by noting that $M_z(\tau+t_w)$ has a term $v(\tau)$ proportional to $\cos(\Delta\omega+\delta)\tau$ from (15-C). This cosine distribution becomes smeared due to diffusion and must be averaged over all δ by applying the integral in (14). However, the self-diffusion of spin-containing molecules will not seriously upset this frequency pattern providing $1/\tau \gg \gamma(dH/dl)l(T)$ (let $T \gg \tau$), where $l(T)$ is the effective distance of diffusion in time T over which a shift in Larmor frequency can occur. The attenuation effect of diffusion upon echoes

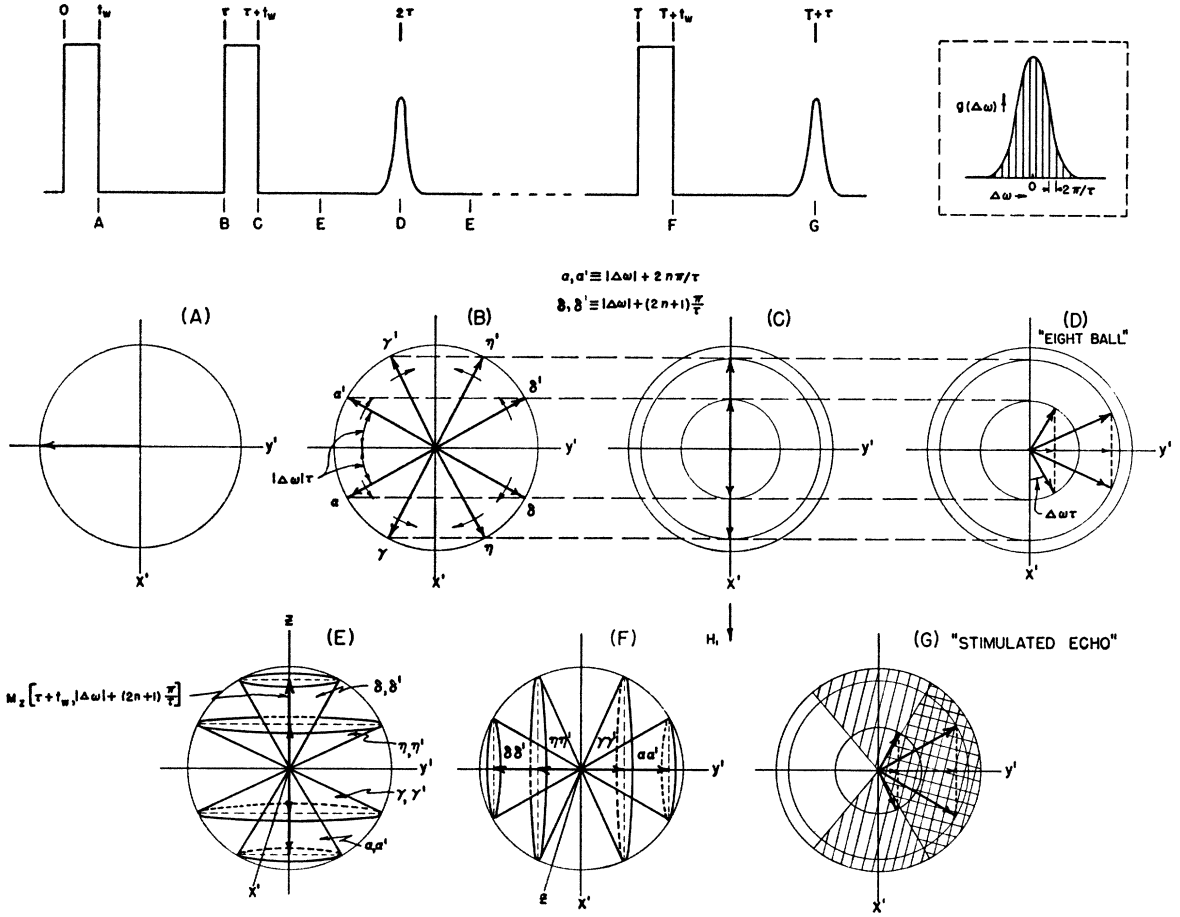

FIG. 6. A vector representation which accounts for the stimulated echo at $t=T+\tau$ is shown under conditions of the special case for the primary echo model in Fig. 1. For a given $|\Delta\omega|$, the symbols α, α' and δ, δ' denote those moments which have Larmor frequencies such that they precess angles $|\Delta\omega|\tau+2n\pi$ and $|\Delta\omega|\tau+(2n+1)\pi$ respectively in time $t=\tau$. n is any integer which applies to frequencies within the spectrum which will lie in a pair of cones corresponding to a specific $|\Delta\omega|$. These cones provide M_z components (after the pulse at τ) which are available for stimulated echo formation after the pulse at T. The shaded area in G indicates the density of moment vectors. The absence of vectors on the $-y'$ side leaves a dimple on the unit sphere.

[16] For $\tau<T<2\tau$ the echo at 2τ is modified and has the coefficient $M_0/4\sin^3\omega_1 t_w$ instead of the one given by (21).

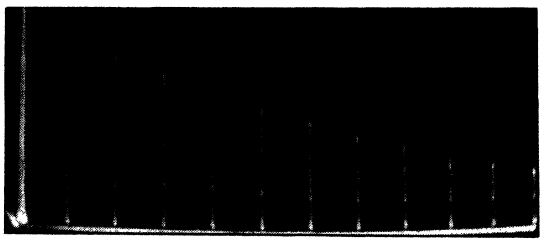

(a)

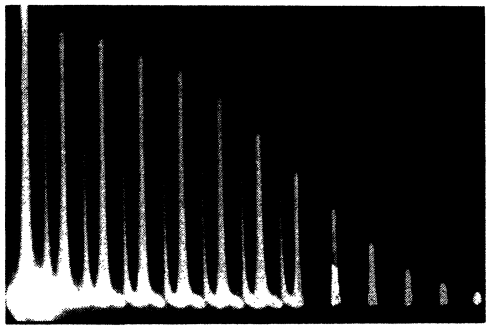

(b)

FIG. 7. A typical exponential plot of stimulated echo amplitudes is shown in the top photograph for protons in H_2O. This is obtained in a manner described for Fig. 3, except that T for the third pulse here is increased by 16/60 sec. intervals while τ is fixed at 0.0039 sec. The measured decay of the envelope is 1.89 sec. which serves as a point on the graph in Fig. 8. The apparent break in intensity in each of the stimulated echoes (seen as vertical traces because of the slow sweep speed) is due to a condition where the echo follows so soon after the stimulating pulse that it superimposes upon the voltage recovery of the receiver detector RC filter.

The bottom photograph indicates approximately an $\exp(-kt^3/3)$ decay law for the primary echo envelope in H_2O. The separation between echoes is 1/60 sec.

whose configuration depends purely upon phase and not frequency is much greater due to the exponential factor $\frac{1}{3}kt^3$ rather than $k\tau^2T$ which occurs only for the stimulated echo.

(F) Measurement of T_1; Qualitative Confirmation of the Diffusion Effect

If the condition $k\tau^2T \ll T/T_1$ is maintained by choosing τ very small, a plot of the logarithm of the stimulated echo maximum amplitude *versus* arbitrary values of T gives a straight line whose slope provides an approximate measure of T_1. In this manner glycerine is found to have a $T_1=0.034$ sec. The self-diffusion coefficient of glycerine is apparently sufficiently small so that T_1 can be measured directly as well as T_2, according to the discussion in III-D. A measured value of $T_2=0.023$ sec. is obtained, which is in substantial agreement with previous measurements.[3,9] The data for T_1 is obtained from oscillographic traces, an example of which is shown in Fig. 7 (top) for protons in distilled water. All relaxation measurements are made at room temperature, at $\omega=30$ Mc. A better value of T_1 is obtainable by plotting $1/T_m$ against τ^2 where T_m is the measured envelope decay time for the stimulated echo which decays as e^{-T/T_m}. A straight line is obtained which has the equation $1/T_m=1/T_1+k\tau^2$, which is seen from the exponential factor in (22-A) where $t=T+\tau$ and $\tau \ll T$. Such a plot is given in Fig. 8 for protons in distilled water (not in vacuum) where the reciprocal of the ordinate intercept gives $T_1=2.3\pm0.1$ sec., in agreement within experimental error with previous measurements.[3,17] Using the value of $D=2\times10^{-5}$ cm^2/sec. for the water molecule,[18] the field gradient, G, calculated from the measured slope is 0.9 gauss/cm, which correlates roughly with the actual gradient over the sample. The gradient is expressed as $G\approx(\Delta H)_{\frac{1}{2}}/d$ where $(\Delta H)_{\frac{1}{2}}$ $\sim$0.2 gauss is measured directly from the resonance absorption line width (or echo width) and $d\sim3$ to 4 mm is the average thickness of the cylindrical sample. In Fig. 7 (bottom) the echo envelope for protons in distilled H_2O is reduced to $1/e$ of its maximum amplitude at $t=(3/k)^{\frac{1}{3}}$, since we neglect the decay due to T_2, which is negligible compared to diffusion. The calculated $(\Delta H)_{\frac{1}{2}}$ here is also in rough agreement with the actual field inhomogeneity present. This agreement with the predicted diffusion law confirms the existence at least of a smooth gradient in H_0 over the sample. If the sample is slightly rotated while r-f pulses are applied to obtain echoes, the echo amplitude is markedly reduced as the spin ensemble rotates into varying field inhomogeneity patterns.

(G) The Echo Beat and Envelope Modulation Effects

It has been found that the exact magnetic resonance frequency of nuclear moments of a given species depends upon the type of molecule in which it is contained. It is apparent that the local magnetic field at the position of the nucleus is shifted from the value of the applied external field by an amount which is too large to be accounted for by the normal diamagnetic correc-

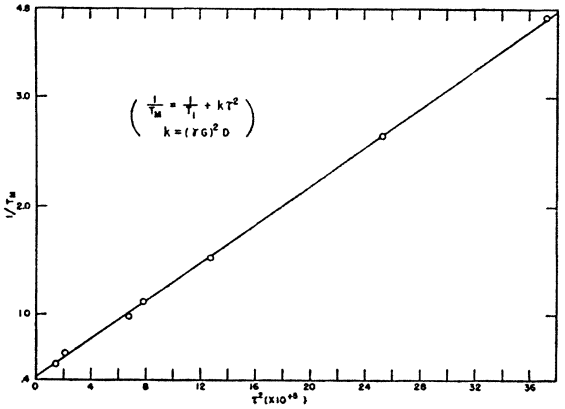

FIG. 8. Stimulated echoe measurement of spin-lattice relaxation time (T_1) of protons in H_2O.

[17] E. L. Hahn, Phys. Rev. **76**, 145 (1949).
[18] W. J. C. Orr and J. A. V. Butler, J. Chem. Soc. 1273 (1935).

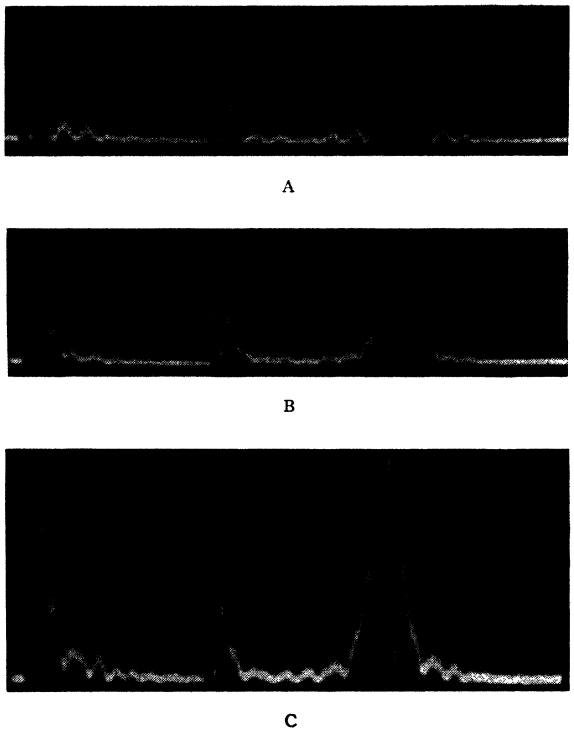

FIG. 9-A-B-C. Heterodyne beat signals for different F^{19} resonance frequencies due to the chemical Larmor shift effect.
(A) $CF_3CCl=CCl_2$ and 1,4 difluoro-benzene ($C_6H_4F_2$) mixture
(B) $CF_3CCl=CCl_2$ and 1,2,4 trifluoro-benzene ($C_6H_3F_3$) mixture
(C) 1, trifluoro-methyl 2,3,6 trifluoro-benzene ($C_6H_2F_3CF_3$)

tion.[19] Ramsey has shown that there exists the possibility of a much stronger field shift[20] due to second-order paramagnetism arising from the type of molecule which contains the nuclear spin. The echo technique reveals simultaneously the presence of two or more groups of resonant nuclei having slightly different Larmor frequencies due to such possible shifts in the local field at the nucleus, providing they are of the order of $(\Delta\omega)_{\frac{1}{2}}/\gamma$ gauss in magnitude. Echoes and free induction decay signals are modulated by beat patterns (Fig. 9) due to the fact that two or more spin groups of one species are contained in the same molecule or different molecules and have non-equivalent molecular environments in the same sample. For example, let ω' and ω'' denote respectively the Larmor frequencies at which the rotating coordinate systems of two spin ensembles may precess, and allow symmetric distribution functions $g'(\Delta\omega')$ and $g''(\Delta\omega'')$ to be a maximum for $\Delta\omega'=\omega_0-\omega'=0$, $\Delta\omega''=\omega_0-\omega''=0$. Therefore, identical echo configurations will result in two frames of reference, each rotating with frequencies ω' and ω'' respectively. The r-f induction is due to the magnetization component $v(\Delta\omega, t)\sin\omega t$ for an individual spin group where $v(\Delta\omega, t)$ is described as in (16) and (17). Integration over all frequencies leading to (20) and (21) provides the following total induction:

$$V(t)=V'(t)\sin\omega'(t-t_1')+V''(t)\sin\omega''(t-t_1'). \quad (23)$$

$V'(t)$ and $V''(t)$ signify the free induction signals due to each of the spin groups alone. The envelope of the echo signal (Fig. 9-A) is given by

$$V(t)_{\max}=[V'(t)^2+V''(t)^2+2V'(t)V''(t)\times\cos(\omega''-\omega')(t-2\tau)]^{\frac{1}{2}}. \quad (24)$$

As typical examples of this effect it has been found that the signals due to F^{19} nuclei in certain organic compounds yield modulation patterns which obey the heterodyne law expressed by (24). In order to observe this effect the condition $2\pi/(\omega''-\omega')\lesssim T_2^*$ must be attained in order to observe at least one period of the modulation within the lifetime T_2^* of an echo or induction decay signal following a pulse. Consequently, a high degree of homogeneity in the magnetic field must be attained in order to get very good resolution; i.e., to resolve very small shifts in Larmor frequency. It appears that this approach to the determination of very small Larmor shifts has a resolution no better than ordinary magnetic resonance absorption methods[1,3] in which the limitation is also due to external field inhomogeneities. However, the echo method is fast and lends itself more conveniently to search purposes in finding these shifts.[21] Somewhat higher resolution than that available by the normal method can be attained beyond the limitation imposed by field inhomogeneities by introducing into the receiver an r-f signal at a frequency somewhere near the Larmor frequencies present. An audio beat modulation appears having an envelope which is modulated in turn by the Larmor shift beat note. These beats can then be more easily distinguished from noise for the condition $2\pi/(\omega''-\omega')\gtrsim T_2^*$ in favorable cases in which the induction signals are sufficiently intense. Periods of the order of $3, 4T_2^*$ may possibly be observed, in which case Larmor shifts as small as 0.01 gauss, of the order of normal diamagnetic shifts, may be detected, assuming a $(\Delta H)_{\frac{1}{2}}\sim 0.05$ gauss is available out of a total field of 7000 gauss. It can be seen from Fig. 9 that the modulation on the echo and decay signals (following r-f pulses) correlate in pattern. It is significant that the pattern on the echo is always symmetric regardless of the spacing τ between the two r-f pulses. This is understandable in view of the fact that two rotating frames of reference, for example, increase in phase difference by $(\omega''-\omega')\tau$ radians between the pulses. The second pulse produces an initial condition such that the two frames

[19] W. E. Lamb, Phys. Rev. **60**, 817 (1941).
[20] This is treated theoretically in a paper in Phys. Rev. **78**, 699 (1950), kindly forwarded to the author in advance of publication by Professor N. F. Ramsey.
[21] One must be careful that the observed modulation is not due instead to a condition where the H_0 magnetic field inhomogeneity pattern over the sample has two or more discrete bumps in it. The modulation will again be symmetric on the echo and can only be distinguished from a true beat effect by moving the sample to a different part of the field in the magnet gap and noting whether or not the modulation disappears or varies in frequency.

of reference now rotate into one another by the same amount and coincide at the time 2τ of the echo maximum. This principle is inherent in the echo effect itself: the phase differences of all moment vectors (with respect to the initial orientation established by the first pulse) are effectively cancelled at the time of the echo maximum. This cancellation is made possible by the second pulse. If no further pulses are applied, the echo at 2τ can never repeat itself, as might be expected, because the "eight-ball" configuration is essentially only a single recurrence of the initial in-phase condition of the moment vectors at $t=t_w$, though not quite the same due to a spread in Larmor frequencies.[22]

Fluorine nuclei in the compounds[23] $CF_3CCl=CCl_2$ and $C_6H_4F_2$ (1,4 difluoro-benzene) give induction signals in separate samples in which no significant beat patterns appear. Weak beats may appear due to other fluorine compound impurities used in the synthesis of these compounds. Figure 9-A indicates the beat which results when these two molecules are mixed in liquid form in a single sample such that two fluorine spin groups are in a one-to-one ratio in concentration. The separate molecules contain fluorine atoms located in equivalent positions and therefore cannot give rise to a beat among themselves. A mixture of the two molecules, having fluorine nuclei which are relatively non-equivalent in molecular environment, now reveals a separation of 1.9 kc in Larmor frequency for the two groups in a field of 7500 gauss. According to (24) the modulation pattern goes to a complete null at this frequency since the mixture is adjusted so that $V'(t) = V''(t)$. By observing the normal resonance absorption signal of this mixture on the oscilloscope, using 30 cycle field modulation, two distinct absorption lines are observed, separated by 1.9 kc on a frequency scale. By using a mixture in which the concentration of one molecule exceeds that of the other, the relative difference in intensity of the absorption lines indicates that the fluorine resonance frequency in $C_6H_4F_2$ lies on the high side relative to that in $CF_3CCl=CCl_2$. It is reasonable to expect this if the charge density of the electronic configuration about the fluorine nuclei in $C_6H_4F_2$, being less than that in $CF_3CCl=CCl_2$, can be correlated with a correspondingly smaller negative magnetic shielding correction. This property appears to exist in all mixtures and single molecules so far investigated in which a distinction between spin groups has been made. Within experimental error, the Larmor

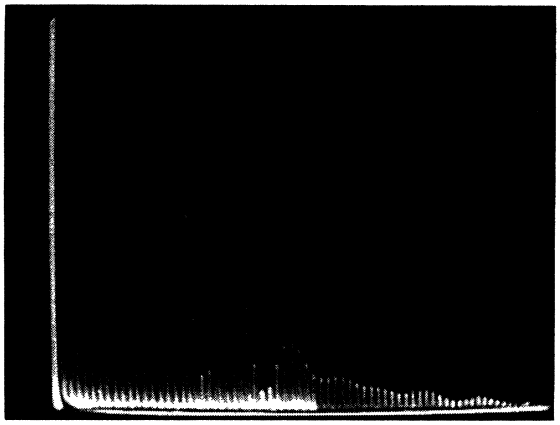

FIG. 10. The echo envelope modulation effect for protons in C_2H_5OH. Paired pulses are applied in the usual manner for obtaining multiple exposures. The echo separation is 1/300 sec. The first echo at the left follows so closely after the r-f pulses that it is not at normal amplitude because of receiver saturation.

frequency shifts observed here appear to be proportional to the applied field, based on measurements made at 7070 and 3760 gauss. Figure 9-B shows the beat pattern due to approximately a one-to-one mixture (in terms of fluorine nuclei) of the compounds 1, 2, 4 trifluoro-benzene and $CF_3CCl=CCl_2$. More than one beat modulation frequency is evident, due obviously to the presence of more than two fundamental spin groups. Figure 9-C shows how a similar complexity in beat pattern arises from a sample of 1-trifluoro-methyl 2, 3, 6 trifluoro-benzene. All observable beat frequencies are of the order of a few kilocycles.

Preliminary studies have been made of another effect which is shown in Fig. 10. The envelope of the normal echo maximum envelope plot is modulated by a beat pattern which is in violation of the normal decay due to self-diffusion and T_2. The envelope shown for C_2H_5OH (period ≈ 0.027 sec.) is an example which is typical for protons in various organic compounds. If the effect is present in the particular substance investigated it is readily observable only if the period of the modulation is shorter than the normal decay time of the echo envelope upon which it is superimposed. Several organic compounds studied so far have been observed to have characteristic periods of the order of 0.1 to 0.01 sec. Modulation patterns in many cases do not contain a single frequency but perhaps several as it appears in C_2H_5OH. The period of the modulation is found in general to be greater than T_2^*, the echo lifetime. This modulation effect cannot be attributed to an interference between several spin groups because the observed echo maximum is always due to the sum of the echo maxima contributed by each of the spin groups alone. This is true regardless of the number of different spin groups present, and therefore the beat frequencies due to such Larmor shifts cannot show up in the envelope of the echo maxima. Within experimental error

[22] It is interesting to note that the configuration at $t=t_w$, namely, $M_{xy}=M_0$, can in principle be exactly repeated at $t=2\tau$ by doubling the second r-f pulse width with respect to the first one which is at the pulse condition $\omega_1 t_w=\pi/2$ (see Fig. 1). Actual experiment indicates that the inhomogeneity in H_1 throughout the sample prevents this from exactly taking place, but shows an increase in the available echo amplitude beyond the optimum amplitude at $\omega_1 t_w=2\pi/3$ (Eq. 21). The stimulated echo at $t=T+\tau$ then nearly disappears.

[23] The fluorine compounds used were kindly provided by Dr. G. C. Finger of the Fluorspar Research Section of the Illinois State Geological Survey, where they were synthesized.

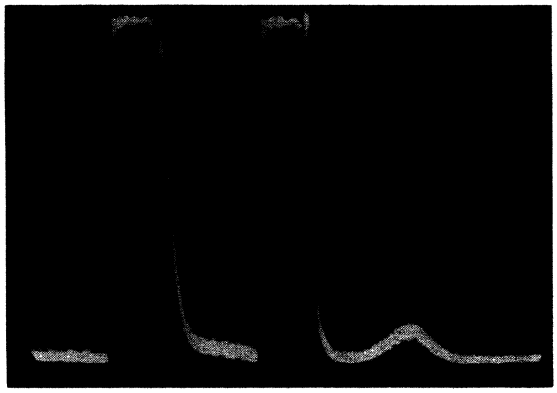

FIG. 11. Free induction signals for protons in paraffin. The echo lasts for $\sim 1.4\times 10^{-5}$ sec. The r-f pulses, about 25 μsec. wide, cause some blocking of the i.f. amplifier. The echo envelope decay time is also of the order of the single echo lifetime.

(five to ten percent) the period of the envelope modulation is found to be inversely proportional to the applied magnetic field. It is possible that an interaction between the nuclear spin and the molecule which contains it causes a periodic reduction of the echo amplitude by a modification of the echo constructive interference pattern. This effect will be treated in a later paper in greater detail.

(H) Free Nuclear Induction in Solids

It has been established in the case of liquids that, if one excludes the effect of diffusion, the lifetime of the nuclear induction decay following a pulse is given by $T_m = T_2T_2^*/(T_2+T_2^*)$, and the single echo lifetime is given by T_2^*. Qualitative observations of free nuclear induction signals due to nuclei in solids, however, indicate that the role played by T_2^* is no longer significant. The ensemble instead precesses in a magnetic field distribution described by a function $G(\delta\omega)$, where $\delta\omega = \omega_0' - \omega'$ and $\omega_0' = \gamma(H_{\text{local}} + H_{\text{magnet}})$. The local field H_{local}, due to lattice neighbors, is superimposed on the externally applied field at the positions of the precessing nuclei. This local field is spread over a width much greater than the width due to the magnet. In one case echoes have been observed for protons in paraffin (Fig. 11) where it appears that the echo and induction decay lifetimes are now given by $\sim 1/(\delta\omega)_{\frac{1}{2}}$ seconds. Extremely intense r-f power is required in order to excite all of the spins over a broad spectrum of Larmor frequencies in a pulse time $t_w \gtrsim 1/(\delta\omega)_{\frac{1}{2}}$ seconds, and therefore the condition $1/t_w,\ \omega_1 \gg (\delta\omega)_{\frac{1}{2}}$ must apply. A striking indication of the predominance of either T_2^* or $1/(\delta\omega)_{\frac{1}{2}}$ is shown by observing how the broad free induction signals from protons in liquid paraffin become very narrow as the paraffin cools and solidifies. It appears that echoes in solids can be observed in principle in a time $\lesssim T_2 \sim 1/(\delta\omega)_{\frac{1}{2}}$, because a given distribution in H_{local} determined by $G(\delta\omega)$ (which now plays the role of $g(\Delta\omega)$ in the case of liquids) is able to last roughly for a time T_2. The local z magnetic field due to neighboring magnetic moments (nuclear spins, paramagnetic ions and impurities) therefore not only depends upon the particular location of these moments with respect to the precessing nucleus, but also upon a time T_2. This time determines how long a given parallel and antiparallel configuration of these neighboring moments can exist with respect to the externally applied field. It follows, therefore, in the case of paraffin, that the stimulated echo, which depends upon frequency memory of the spin distribution, cannot be observed out to times $T+\tau \sim T_1 = 0.01$ sec., where $T_1 \gg T_2$.

Although the Bloch theory is highly successful in accounting for the echo effect in liquids where T_1 and T_2 are introduced in a phenomenological way, it must be understood in this theory that the predicted natural resonance line shapes will always be described by a damped oscillator resonance function (Lorentz) in the steady state. This corresponds to the observed exponential decay of free induction signal amplitudes in the transient case. This concept does not necessarily apply in general, especially as regards magnetic resonance line shapes in solids in the steady state. It remains to be shown that the properties of free nuclear induction signals in solids are explained by a transient analysis which gives results equivalent to the general steady state treatment formulated by Van Vleck[24] and others.[3,25]

With further refinements in technique for obtaining a sufficiently fast response of the r-f circuits to very short r-f pulses of large intensity (t_w of the order of microseconds at $H_1 \sim 20$ to 100 gauss), it may be possible to obtain informative data from free nuclear induction signals in solids which have a T_2 of the order of 10^{-5} to 10^{-6} seconds. It will be of profit to investigate the induction decay which follows single pulses (already found for protons in powdered crystals of NH_4Cl, $(NH_4)_2SO_4$, $MgSO_4 \cdot 7H_2O$ and for F^{19} in CaF_2) without the attempt to observe echoes.

IV. EXPERIMENTAL TECHNIQUE

The block diagram in Fig. 12 indicates the necessary components for obtaining the echo effect. All features of the sample, inductive coil, and methods of coupling from the oscillator and to the receiver are typical of nuclear induction techniques and have been discussed in detail elsewhere. A great simplification is introduced here because only a single LC tuned circuit is necessary. However, in the case where a narrow band receiver is used ($\sim$8 kc) in place of a very broad band i.f. strip ($\sim$5 Mc) and where r-f pulses are particularly intense, it is convenient to use a bridge balance in order to minimize overloading of the receiver. Two methods have been used to provide r-f power in the form of pulses. A method best suited for r-f amplitude and frequency stability employs a 7.5 Mc crystal-controlled

[24] J. H. Van Vleck, Phys. Rev. **74**, 1168 (1948).
[25] G. E. Pake, J. Chem. Phys. **16**, 327 (1948).

oscillator whose frequency is quadrupled to 30 Mc and amplified r-f power is then gated through stages whose grids are biased by square wave pulses from a one shot multivibrator controlled in turn by timer pulses. This method is essential for studies of the phases of various echo signals and other effects. The crystal maintains a source of coherent r-f oscillations which can be used to heterodyne weakly with the nuclear signal that has a phase determined initially by these oscillations in the form of intense pulses. The phases of the resulting audio beat frequency oscillations seen superimposed on the echoes then yield certain interesting proofs.

(a) The phase of the audio modulation on all echoes is invariant to any time variation in the spacing between r-f pulses. With respect to a fixed reference in a rotating coordinate system, all echoes form a resultant which is constant in direction due to the fact that the accumulated phase differences before the r-f pulse (at $t=\tau$) are exactly neutralized after it (referring to discussion in III-G).

(b) The negative sign of the "image echo" term (Eq. 22-B) signifies that the resultant of this signal is 180° out of phase relative to the resultants of all other echoes formed before or after it. This is borne out by the fact that the phase of the observed audio modulation on the image echo is exactly 180° out of phase with respect to the modulation pattern on all other echoes. Otherwise, the modulation patterns appear to be identical.

(c) Echoes at $t=2\tau$ are observed not to fluctuate in amplitude when $\tau<T_2^*$ due to the fact that the r-f is coherent for successive pulses, and the phase of the moment configuration prior to the r-f pulse at τ has a definite relationship with respect to the phase of the echo which follows.

With the above method, precautions must be taken to prevent r-f power leakage to the sample during the absence of pulses. The necessity for this precaution is eliminated by turning on and off a high power oscillator (by gating the oscillator grid bias, Fig. 13) which drives the LC circuit directly. This method, although not as stable, makes available higher r-f power, and the ability to vary the driving frequency ω is convenient. Although r-f pulses are produced now in random phase, experimental results are the same as long as $\tau\gg T_2^*$. Both

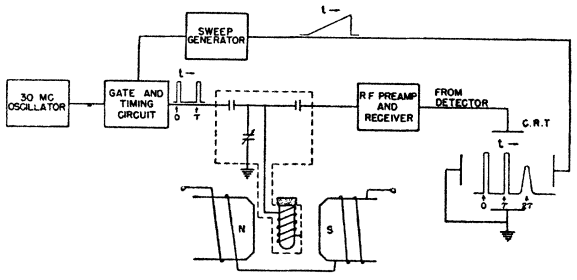

FIG. 12. Arrangement for obtaining spin echoes.

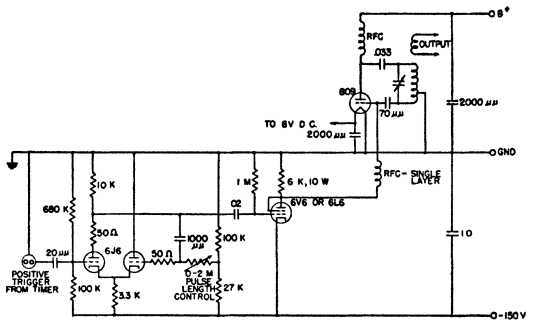

FIG. 13. Gated oscillator.

pulse methods combined provide pulses of $t_w\sim 20$ μsec. to a few milliseconds and $H_1\sim 0.01$ to 50 gauss.

In order to obtain accurate and reproducible data with echoes it is necessary that the dc magnetic field be held constant to at least one part in 10^5 over the length of time during which a set of echo data is being photographed. One might say that some field drift is tolerable within the limits set by the condition $\omega_1\gg(\Delta\omega)_{\frac{1}{2}}$. However, it is advisable even to guard against field drifts less than H_1 gauss because the Fourier amplitudes of all r-f frequency components which resonate with the given Larmor spin frequencies will vary to some degree as the dc field varies. In cases where the decay of echoes is plotted for nuclei in liquids having a long T_1 (several seconds for protons in most organic liquids) and where maximum available signal is desired, the spins must be allowed to return to complete thermal equilibrium between applications of paired pulses. Therefore, if one waits at least five half-lives to obtain a plot such as is shown in Fig. 10, a total time of 17 minutes is required during which the magnetic field must not drift appreciably. In order to minimize the effect of slow field drifts it is convenient to apply paired pulses at a repetition rate whose period is some constant fraction of T_1. During this period the operator has sufficient time to adjust timer switches (reset switches on a conventional scalar unit[17]) in order to provide increasing integers of time between the two pulses. The sample is therefore partially saturated at a level which is practically constant when the pulses are applied, although a small but negligible variation in the level of saturation is introduced as the time τ is systematically increased. The over-all signal to noise ratio of the pattern is reduced but data can be recorded at a convenient speed.

For these experiments the magnetic field is stabilized by means of a separate proton resonance regulator[26] which monitors practically the same magnetic field which is present at the echo sample. The regulator resonance sample is located in the same magnet gap and is subjected to 30 Mc r-f power which is well shielded from the experiment sample. The regulator sample is placed in the inductance of the tuned circuit

[26] To be discussed in a later paper.

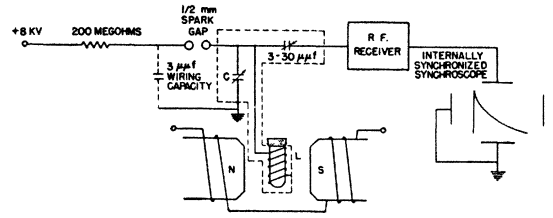

FIG. 14. Simple spark method for obtaining free nuclear induction decay signals.

of a transitron oscillator. A sinusoidally vibrating reed capacitively modulates the frequency of this oscillator within the line width of the regulator proton resonance. When the magnetic field is brought into the resonance value it is locked in and controlled by the regulator. The transitron oscillator r-f voltage level decreases due to resonance absorption and is modulated at the frequency of the vibrating reed. A discriminator circuit utilizes this signal to control a correction current to the magnet in a conventional manner.[27]

In Fig. 14 a sparking technique is noted purely for its novel features of simplicity in demonstrating, qualitatively, free nuclear induction decay signals directly following single random r-f pulses. The spark generated across the gap contains essentially all frequencies and excites for a very short time the tuned circuit in which the sample is located. After the spark extinguishes, the sample in the inductive coil transmits a decaying r-f induction signal to the receiver at the Larmor frequency determined by H_0. Capacitor C needs adjustment such that the tank circuit will resonate approximately in the region of the Larmor frequency (with no spark). Signals can be obtained over a broad range of H_0 without requiring a retuning of C. The observed signal, of course, has random amplitudes since the r-f energy transferred by the sparks is random within a certain range.

[27] M. Packard, Rev. Sci. Inst. **19**, 435 (1948).

V. CONCLUDING REMARKS

Simple principles of the free nuclear induction technique have been described and tested, principally with proton and fluorine (F^{19}) signals in liquids. Data which is made available by this technique is to be presented later in more systematic detail. The echo technique appears to be highly suitable as a fast and stable method in searching for unknown resonances. Intense pulses of H_1 provide a broad spectrum of frequencies. This makes possible the observation of free induction signals far from exact resonance. Echo signals have proved useful for the measurement of relaxation times under conditions where interference effects (microphonics, thermal drifts, oscillator noise) encountered in conventional resonance methods are avoided. The self-diffusion effect in liquids of low viscosity offers a means of measuring relative values of the self-diffusion coefficient D, a quantity which is very difficult to measure by ordinary methods. It is of technical interest to consider the possibility of applying echo patterns as a type of memory device.

The formal analysis of the signal-to-noise ratio of the echo method is nearly identical to the treatment already given by Torrey with regard to transient nutations.[9] However, a great practical improvement in eliminating noise is available with the echo technique which cannot be assessed from formal analysis; namely, that H_1 is absent during the observation of nuclear signals, and noise or hum that may be introduced by the oscillator and associated bridge components is avoided.

The author wishes to thank Professor J. H. Bartlett for his counsel in carrying out this research, and is grateful to Dr. C. P. Slichter for the benefit derived from many clarifying discussions with him regarding this work. The author is indebted to H. W. Knoebel for his excellent design and construction work on the electronic apparatus.

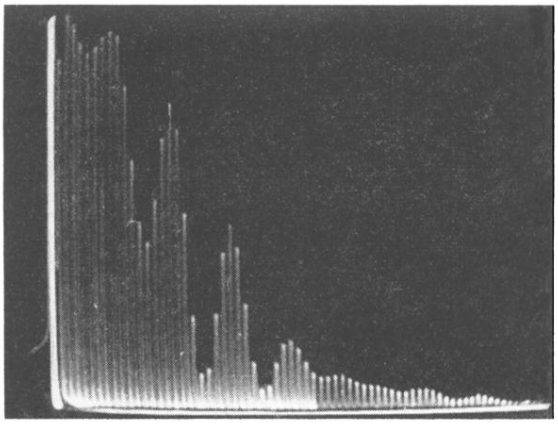

FIG. 10. The echo envelope modulation effect for protons in C_2H_5OH. Paired pulses are applied in the usual manner for obtaining multiple exposures. The echo separation is 1/300 sec. The first echo at the left follows so closely after the r-f pulses that it is not at normal amplitude because of receiver saturation.

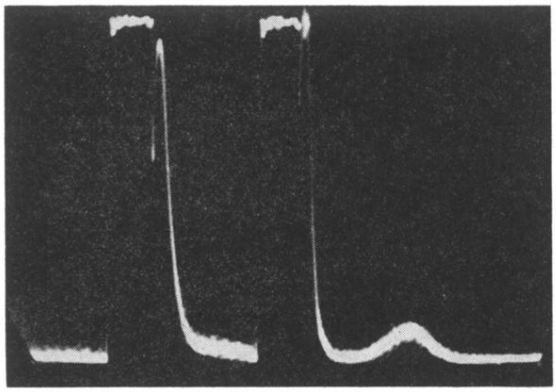

FIG. 11. Free induction signals for protons in paraffin. The echo lasts for $\sim 1.4 \times 10^{-5}$ sec. The r-f pulses, about 25 μsec. wide, cause some blocking of the i.f. amplifier. The echo envelope decay time is also of the order of the single echo lifetime.

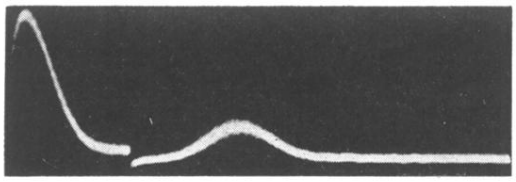

a

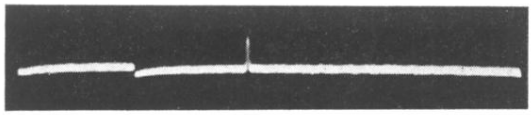

b

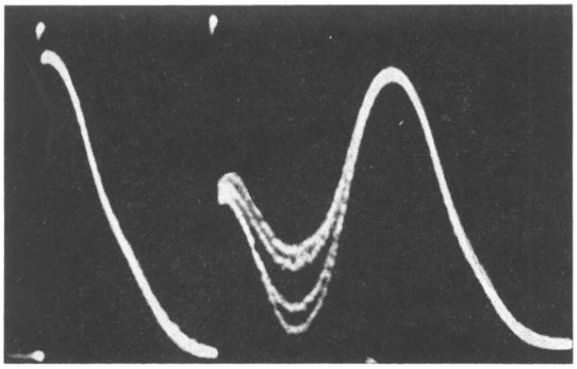

c

FIG. 2. Oscillographic traces for proton echoes in glycerine. The two upper photographs indicate broad and narrow signals corresponding to H_0 fields of good and poor homogeneity. The pulses, scarcely visible, are separated by 0.0005 sec. The induction decay following the first pulse in the top trace has an initial dip due to receiver saturation. The bottom photograph shows random interference of the induction decay with the echo for several exposures. The two r-f pulses are phase incoherent relative to one another.

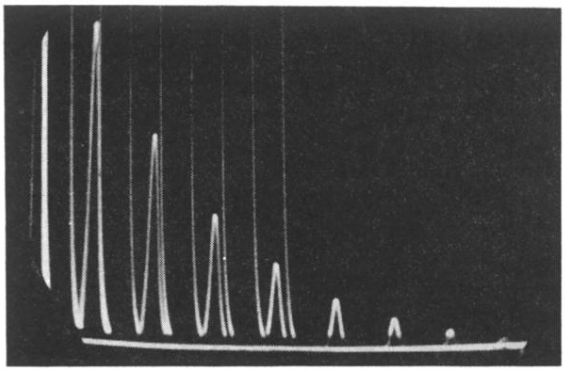

FIG. 3. Multiple exposures of proton echoes in a water solution of $Fe(NO_3)_3$ (2.5×10^{18} Fe^{+++} ions/cc). The faint vertical traces indicate paired pulses which are applied at time intervals $\gg T_2$, with the first pulse of each pair occurring at the same initial position on the sweep. For each pulse pair the interval τ is increased by 1/300 sec. The echoes are spaced 2/300 sec. apart and the measured decay time constant of the echo envelope gives $T_2=0.014$ sec.

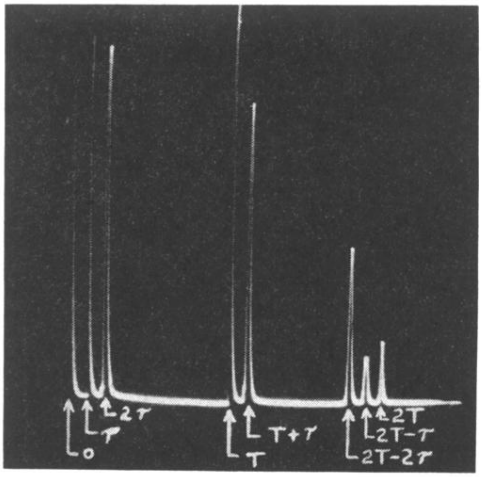

a

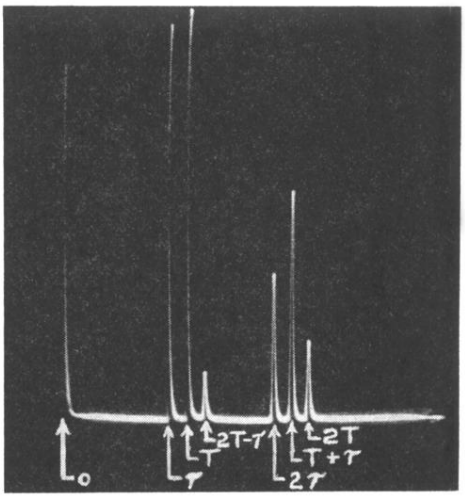

b

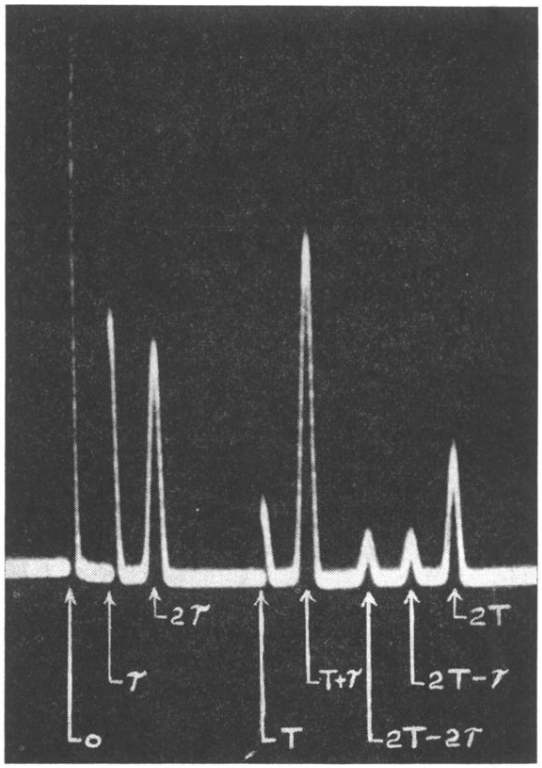

c

FIG. 5. Proton echo patterns in H_2O resulting from three applied r-f pulses. The pulses are visible in the upper two traces, and have a width $t_w \sim 0.5$ msec. In the upper trace $\tau = 0.008$ sec., $T = 0.067$ sec., and for the second trace $\tau = 0.046$ sec. and $T = 0.054$ sec. The bottom photograph shows a similar pattern for the case $T > 2\tau$ where induction decay signals can be seen following very short invisible r-f pulses. Saturation of a narrow band communications receiver, used in the case of the upper two traces, prevents the observation of these signals, whereas a wide band i.f. amplifier makes this observation possible in the bottom photograph.

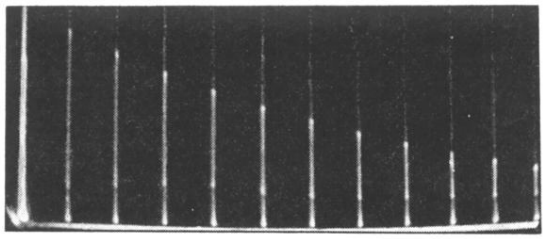

(a)

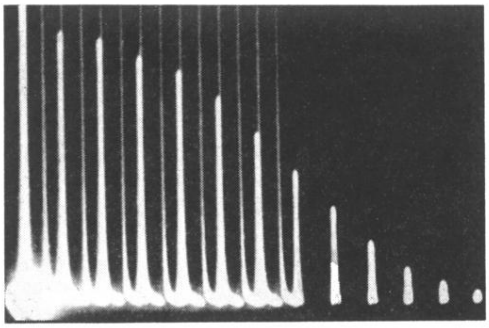

(b)

FIG. 7. A typical exponential plot of stimulated echo amplitudes is shown in the top photograph for protons in H_2O. This is obtained in a manner described for Fig. 3, except that T for the third pulse here is increased by 16/60 sec. intervals while τ is fixed at 0.0039 sec. The measured decay of the envelope is 1.89 sec. which serves as a point on the graph in Fig. 8. The apparent break in intensity in each of the stimulated echoes (seen as vertical traces because of the slow sweep speed) is due to a condition where the echo follows so soon after the stimulating pulse that it superimposes upon the voltage recovery of the receiver detector RC filter.

The bottom photograph indicates approximately an $\exp(-kt^3/3)$ decay law for the primary echo envelope in H_2O. The separation between echoes is 1/60 sec.

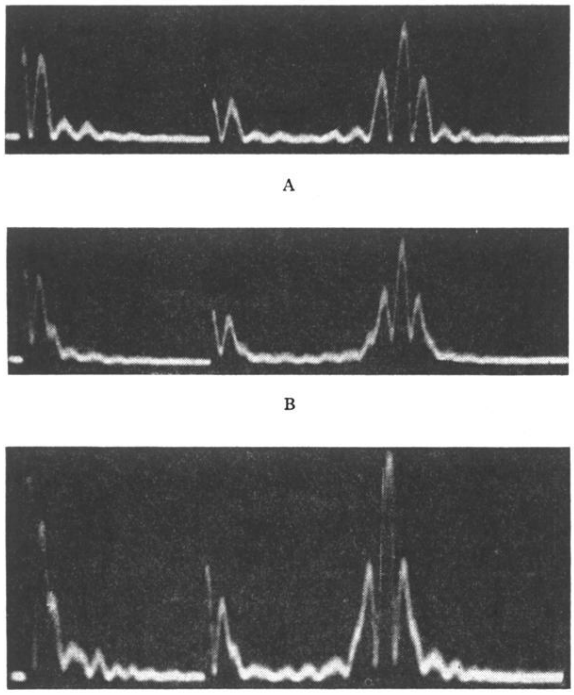

A

B

C

FIG. 9–A–B–C. Heterodyne beat signals for different F^{19} resonance frequencies due to the chemical Larmor shift effect.
(A) $CF_3CCl=CCl_2$ and 1,4 difluoro-benzene ($C_6H_4F_2$) mixture
(B) $CF_3CCl=CCl_2$ and 1,2,4 trifluoro-benzene ($C_6H_3F_3$) mixture
(C) 1, trifluoro-methyl 2,3,6 trifluoro-benzene ($C_6H_2F_3CF_3$)